BIOCHEMISTRY
including biophysical chemistry & molecular biology

Article

pubs.acs.org/biochemistry

Metabolic Function for Human Renalase: Oxidation of Isomeric Forms of β-NAD(P)H that Are Inhibitory to Primary Metabolism

Brett A. Beaupre, Matt R. Hoag, Joseph Roman, F. Holger Försterling, and Graham R. Moran*

Department of Chemistry and Biochemistry, University of Wisconsin-Milwaukee, 3210 North Cramer Street, Milwaukee, Wisconsin 53211-3209, United States

Supporting Information

ABSTRACT: Renalase is a recently identified flavoprotein that has been associated with numerous physiological maladies. There remains a prevailing belief that renalase functions as a hormone, imparting an influence on vascular tone and heart rate by oxidizing circulating catecholamines, chiefly epinephrine. This activity, however, has not been convincingly demonstrated in vitro, nor has the stoichiometry of this transformation been shown. In prior work we demonstrated that renalase induced rapid oxidation of low-level contaminants of β-NAD(P)H solutions (Beaupre, B. A. et al. (2013) *Biochemistry 52*, 8929−8937; Beaupre, B. A. et al. (2013) *J. Am. Chem. Soc. 135*, 13980−13987). Slow aqueous speciation of β-NAD(P)H resulted in the production of renalase substrate molecules whose spectrophotometric characteristics and equilibrium fractional accumulation closely matched those reported for α-anomers of NAD(P)H. The fleeting nature of these substrates precluded structural assignment. Here we structurally assign and identify two substrates for renalase. These molecules are 2- and 6-dihydroNAD(P), isomeric forms of β-NAD(P)H that arise either by nonspecific reduction of β-NAD(P)$^+$ or by tautomerization of β-NAD(P)H (4-dihydroNAD(P)). The pure preparations of these molecules induce rapid reduction of the renalase flavin cofactor (230 s^{-1} for 6-dihydroNAD, 850 s^{-1} for 2-dihydroNAD) but bind only a few fold more tightly than β-NADH. We also show that 2- and 6-dihydroNAD(P) are potent inhibitors of primary metabolism dehydrogenases and therefore conclude that the metabolic function of renalase is to oxidize these isomeric NAD(P)H molecules to β-NAD(P)$^+$, eliminating the threat they pose to normal respiratory activity.

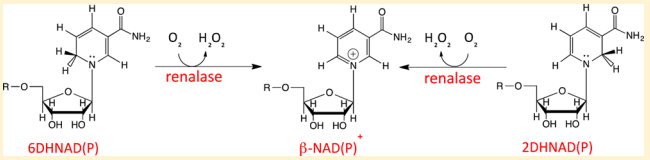

Renalase is a flavoprotein that has been proposed to be an enzyme/hormone produced by the human kidney to attenuate blood pressure and slow the heart.[1] It has been asserted that this physiological response is achieved by catabolizing circulating catecholamines.[2] However, this claimed activity has never been convincingly demonstrated, and a number of factors portend a more prevalent metabolic role for renalase. The first is that renalase transcripts have been detected in numerous mammalian tissues.[3−5] The second is that the X-ray crystal structure of renalase has revealed a unique constellation of conserved residues about an active site flavin isoalloxazine ring that form a structural motif that is identifiable in homologues as far removed as the cyanobacteria.[6,7] Despite numerous reports of physiological relevance, a definitive catalytic reaction for renalase has remained elusive.[8−16] The most persistent claim is that renalase acts as the third monoamine oxidase (MAO C), oxidizing and cyclizing epinephrine and requiring NADH as a reductant to form the aminochrome molecule adrenochrome.[13,17] The reported rates for this conversion, however, are exceedingly slow, and the apparent odd stoichiometry of this reaction, in which four electrons are mobilized, has not been established.

In prior work, we identified fleeting minor contaminants of β-NAD(P)H solutions as substrates for renalase. These molecules induced rapid reduction of the active site flavin that is then reoxidized by reduction of dioxygen. Product analysis indicated β-NAD(P)$^+$ and hydrogen peroxide as products in 1:1:1:1 stoichiometry leading to the conclusion that renalase is an oxidase. On the basis of both spectrophotometric characteristics and aqueous equilibrium proportions, we erroneously proposed that the substrates for renalase were the α-anomers of NAD(P)H[7,18−20] and that the function of renalase was therefore to oxidize and epimerize α-NAD(P)H anomers to avoid an inexorable loss of cellular redox currency as α-NAD(P)$^+$ (molecules that have no known metabolic role in mammalian metabolism). This proposed activity seemed to satisfy a long-standing conundrum whereby despite reported lower reduction potentials for α-anomers, α-NAD(P)$^+$ molecules are not observed to accumulate to any significant level in normal metabolism.[21]

The purpose of this article is to correct the renalase literature, provide direct evidence for the structure of the renalase substrate(s) molecules described in our prior reports, and link these molecules to an apparent important metabolic role for the activity observed. In this study we show that the substrate(s) for renalase are 2-dihyhdroNAD (2DHNAD(P)) and 6-dihydroNAD (6DHNAD(P)), both of which are isomeric forms of β-NAD(P)H where the hydride equivalent resides on either the 2 or the 6 position of the nicotinamide instead of the

Received: October 28, 2014
Revised: December 11, 2014
Published: December 22, 2014

DOI: 10.1021/bi5013436
Biochemistry 2015, 54, 795−806

Scheme 1

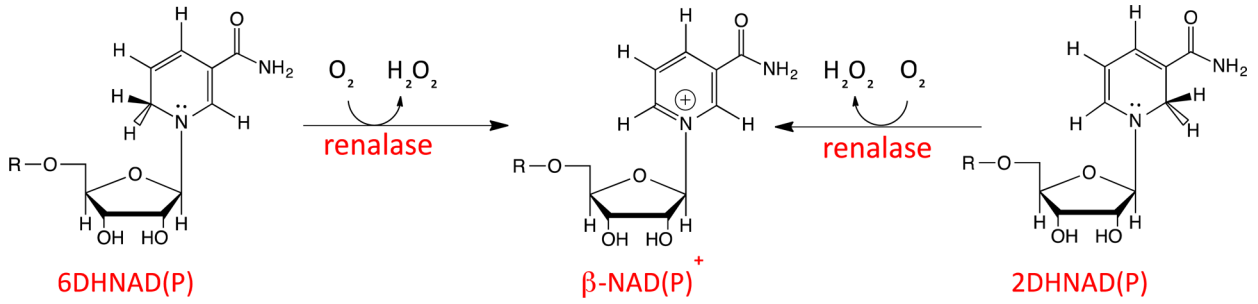

native 4 position. These molecules arise from nonspecific (nonenzymatic) reduction of β-NAD(P)$^+$ or tautomerization of β-NAD(P)H and can inhibit multiple dehydrogenase enzymes of primary metabolic pathways. Renalase would therefore appear to alleviate this inhibition by oxidizing 2DHNAD(P) and 6DHNAD(P) to form β-NAD(P)$^+$ (Scheme 1).

MATERIALS AND METHODS

Materials. β-NADH (disodium salt, trihydrate) was obtained from Amresco. β-NAD$^+$, oxaloacetate, (±)-α-lipoamide, and lactate dehydrogenase (LDH) (rabbit muscle) were each sourced from Sigma-Aldrich. Sodium borohydride, potassium phosphate (mono and dibasic), β-mercaptoethanol, and pyruvate were from Acros. Deuterium oxide was from Cambridge Isotopes. Sep-Pak cartridges were purchased from Waters. Competent NEB5α and BL21 DE3 *Escherichia coli* cells were obtained from New England Biolabs. Q-sepharose was from Bio Rad. Lipoamide dehydrogenase (DLD) (porcine heart) was from Calzyme.

Malate dehydrogenase (MDH) was cloned from *E. coli*. Genomic DNA was isolated from 100 mL of log-phase cells ($OD_{600\ nm} \approx 0.5$) using a Qiagen Genomic DNA preparation kit and protocol. The MDH gene was amplified using oligonucleotides complementary to the 3′ and 5′ ends of the gene that incorporated respective Nde I and Xho I restriction sites (5′-ATTATTATTATT**CATATG**AAAGTCGCAGTCCTCGCGT-3′, 5′-TTTTTTTTTTTTTTT**CTGGAGTTATTA**CTTATTAACGAACTTCGCC-3′; start and stop codons are depicted bolded and restriction sites underlined). The amplified gene was then digested with the above two restriction enzymes and ligated with pET17b plasmid that had been digested in the same way. The ligation was then transformed into competent NEB5α *E. coli* cells and plated onto Luria−Bertani (LB) agar, 100 μg/mL ampicillin. Transformant cultures prepared from individual colonies were grown in LB broth, 100 μg/mL ampicillin and were screened for the correct plasmid insert by agarose gel electrophoresis. Plasmid DNA from each transformant was prepared using the Qiagen Mini-prep kit and protocol followed by digestion with Nde I and Xho I restriction enzymes. The plasmid from verified cell lines were then prepared in sufficient quantity for DNA sequencing using the Qiagen Midi-prep kit and protocol. After sequence confirmation the plasmid, pECMDH, was then transformed into competent BL21(DE3) *E. coli*. A single colony was selected and grown in LB broth medium containing 100 μg/mL ampicillin. Cells from this culture were harvested in early log phase and mixed with 0.22 μm filter sterilized glycerol to a final concentration of 20% v/v and stored as 1 mL aliquots at −80 °C.

MDH was expressed and purified by thawing cell stocks and plating 100 μL per plate onto LB agar plates (100 μg/mL ampicillin) and grown at 37 °C for 16 h. The lawn of cells from two plates was then resuspended into 10 mL of LB broth and used as an inoculum for 1 L LB broth culture (100 μg/mL ampicillin) prewarmed to 37 °C. The cell culture was then shaken at 220 rpm, and the temperature was maintained at 37 °C. When the density of the culture reached $OD_{600\ nm} \approx 1.0$, 0.1 mM isopropyl-β-thiogalactopyranoside (IPTG) was added to induce overexpression of the MDH protein. After 2 h the culture was harvested by centrifugation at 4000*g* in an RC-3C Sorvall centrifuge, and the cell pellet was resuspended in 20 mL of ice-cold 20 mM HEPES buffer, 2 mM β-mercaptoethanol (βME), pH 7.0. All subsequent methods maintained the temperature of the sample at 4 °C, unless otherwise noted. The cell slurry was then sonicated for a total of 5 min at 20 W using a Branson sonicator fit with a blunt tungsten tip. The resulting sonicate was then centrifuged at 15600*g* for 30 min using an Eppendorf 5804R centrifuge. The supernatant was then brought to 1.5% streptomycin over a period of 20 min and centrifuged at 12850*g* for 10 min. The supernatant obtained was decanted and brought to 45% ammonium sulfate saturation over 25 min and centrifuged again at 12850*g* for 10 min. The supernatant was retained and brought to 75% ammonium sulfate saturation over a period of 25 min and centrifuged at 12850*g* for 10 min. The pelleted protein was then redissolved in 20 mM HEPES, 2 mM βME, pH 7.0 (100 mL per liter of culture) and loaded onto a 2.5 × ~25 cm Q-sepharose column at a flow rate of 2 mL/min. Pure MDH protein was then eluted using a linear gradient to 200 mM NaCl spanning a volume of 400 mL supplied from a Biorad Biologic LC chromatographic system. The MDH obtained was then concentrated using 15 mL Amicon, 10 kDa nominal molecular weight cutoff centrifugal concentrator and stored at −80 °C. The pure enzyme was quantified using the calculated extinction coefficient for 280 nm of 6085 M^{-1} cm^{-1}.[22]

The gene for *Saccharomyces cerevisiae* old yellow enzyme (OYE, isoform 1) cloned into the Nde I and Xho I restriction sites of pET28a was obtained from Enzymax as an *E. coli* XL-1 blue transformant culture. Cloning into the Nde I restriction site fuses the OYE1 gene to an N-terminal His-Tag. A 50 μL aliquot of these cells was used to make cell stocks by culturing in 20 mL of LB broth (25 μg/mL kanamycin) incubated at 37 °C with shaking at 220 rpm for 6 h. Cells from this culture were stored in sterile 20% glycerol at −80 °C. Plasmid (pSCOYE) was prepared from 5 mL cultures of these cells using the Qiagen mini-prep kit and protocol and transformed into *E. coli* BL21(DE3) and prepared as cell stocks from a single colony as described above for pECMDH plasmid. OYE was expressed and purified by spread plating onto LB agar (25 μg/mL

DOI: 10.1021/bi5013436
Biochemistry 2015, 54, 795−806

kanamycin, 100 μL of cells per plate) and incubating at 37 °C for 20 h. The lawn of cells from two plates was resuspended in ∼20 mL of LB broth and used as an inoculum for a 1 L culture of LB broth (25 μg/mL kanamycin). Expression of the OYE protein and harvesting of the cells proceeded in a manner identical to that described above for *E. coli* MDH.

To prepare pure OYE the harvested cells were resuspended 20 mL/L of culture, 20 mM HEPES pH 7.5 and sonicated for ∼10 min at 20 W. The lysed cell slurry was then centrifuged at 15600*g* for 30 min, and the supernatant (∼25 mL/L of culture) was then loaded onto a Talon cobalt affinity column at a flow rate of 1 mL/min, and the column was washed with 200 mL of 50 mM HEPES, 10 mM imidazole, pH 7.5. OYE was then eluted with a 400 mL linear gradient to 50 mM HEPES, 300 mM imidazole, pH 7.5 using a Biorad Biologic liquid chromatography device. Fractions containing OYE activity were then pooled, and the buffer was exchanged to 10 mM potassium phosphate buffer, pH 7.5 using an Amicon 15 mL, 10 000 nominal molecular weight cutoff filter/concentrator. The pure OYE obtained was then aliquoted and stored at −80 °C. OYE was quantified using the 461 nm extinction coefficient of the flavin cofactor (10 400 M^{-1} cm^{-1}) that was determined using an SDS denaturation method based on the extinction coefficient of free flavin.[18]

Preparation, Separation, and Analysis of 2- and 6DHNAD. 2- and 6DHNAD were prepared by reduction of β-NAD^+. The ratio of reactants used was developed empirically such that the fractional accumulation of 2DHNAD (the less stable of the products) was comparable to that of 6DHNAD and β-NADH (4DHNAD). Initially, a 37 mM sodium borohydride solution was prepared in 20 mM potassium phosphate titrated to pH 11. A 200 μL aliquot of this solution was then added to a freshly prepared 15.5 mM solution of β-NAD^+ in 100 mM potassium phosphate pH 7.5. Analytical high-pressure liquid chromatography (HPLC) separation of the products of β-NAD^+ reduction was achieved using an Xterra C18 reverse phase column (4.6 × 150 mm, 3.5 μM particle size) run isocratically at 0.5 mL/min in 10 mM potassium phosphate buffer pH 7.5. Purification of 2- and 6DHNAD was achieved by preparative HPLC. The partially reduced β-NAD^+ solution was injected (50−500 μL) onto a Phenomenex reverse-phase phenyl HPLC column (21.2 × 250 mm) run isocratically at 5 mL/min with a mobile phase of 10 mM potassium phosphate, pH 7.5. Both the analytical and preparative columns were coupled to a Waters 600E pump and Waters 2487 dual wavelength detector, and the elution of component species was observed simultaneously at 260 and 340 (or 394) nm. To prepare samples for nuclear magnetic resonance (NMR) and mass spectrometry, reduced products were collected individually into 400 mL glass vessels immersed in liquid nitrogen. The pure dilute solutions were then thawed and desalted at 4 °C by loading onto a 35 cc C18 Sep-Pak cartridge (Waters) and eluted with a 200 mL gradient from 10 mM to 0 mM potassium phosphate pH 7.0 using a Biorad Biologic liquid chromatography device. The desalted samples were then dried by lyophilization (in order to minimize ambient temperature decomposition, the lyophilization vessels were embedded in ice throughout). Each of the desalted, dry, and pure reduction products was then dissolved in cooled deuterium oxide (D_2O) and used immediately for NMR or dissolved in cooled water for mass spectrometry. For kinetic studies, the product identified as 6DHNAD was collected, desalted, concentrated, and redissolved in D_2O as described above and stored at −80 °C. The product identified as 2DHNAD could not be stored due to pronounced instability and was instead collected from the HPLC and used immediately (within 1−5 min).

Spectrophotometric Quantification of NAD Molecules. The concentration β-NADH was determined using the published 340 nm extinction coefficient of 6220 M^{-1} cm^{-1}.[19] Dihydronicotinamide chromophore extinction coefficients for 2- and 6DHNAD (and the 260 nm extinction coefficient for β-NAD^+) were obtained using renalase to oxidize both molecules to β-NAD^+. Initially, the spectrum of each HPLC purified molecule (70−90 μM) was acquired using a Hewlett-Packard 8453 spectrophotometer. The 2- and 6DHNAD were then oxidized to β-NAD^+ by adding 30 nM renalase. 4DHNAD (β-NADH) prepared in the same manner was oxidized to β-NAD^+ by the addition of 30 nM OYE. Under these conditions complete oxidation was achieved in 2−3 min. The pairs of fully reduced and fully oxidized spectra obtained from each reaction were then multiplied by the factor required to normalize the β-NAD^+ spectra, and then all spectra were multiplied by the factor required to convert the β-NADH spectrum to equal its known extinction coefficient at 340 nm. This method gave extinction coefficients of ε_{394nm} = 5360 M^{-1} cm^{-1} for 2DHNAD, ε_{345nm} = 6580 M^{-1} cm^{-1} for 6DHNAD (cf. α-NADH ε_{345nm} = 6170 M^{-1} cm^{-1}) and ε_{260nm} = 18 800 M^{-1} cm^{-1} for β-NAD^+.

Mass Spectrometry. For both 2- and 6DHNAD, an HPLC purified and C^{18} Sep-Pak desalted sample (∼50−100 μM, prepared as described above) was collected. This sample was injected via a Shimadzu LC-2010C liquid chromatography system onto a Shimadzu 2020 mass spectrometer. In each case, 10 μL of sample was delivered in a 1:1 mixture of water and methanol. Data were collected in negative ion mode in the mass range 100−800. This procedure was also followed for β-NADH, β-NAD^+ as controls.

Nuclear Magnetic Resonance. NMR experiments were carried out at 280 K in D_2O solvent using a Bruker DRX-500 NMR spectrometer equipped with a triple axis gradient inverse (BBI) probe operating at a frequency of 499.832389 MHz for proton and 125.6936644 MHz for ^{13}C. Chemical shifts are reported relative to the methyl signal of the sodium salt of 3-(trimethylsilyl) propanesulfonic acid using the residual HDO signal as indirect reference. One-dimensional experiments were performed by accumulating 128 scans using a spectral width of 10330 Hz (^1H) and 20161 Hz (^{31}P) and using relaxation delays of 1 s and 3 s, respectively. For a typical gradient selected DQF−COSY experiment 960 t_1 increments with 32 transients of 2048 points covering a spectral width of 5000 Hz were acquired. $^1H\{^{13}C\}$-HSQC spectra were acquired with gradient selection and multiplicity editing, using 730 t_1 increments with 64 transients of 1600 points each, covering a spectral width of 5000 and 22624 Hz in f2 and f1, respectively. A mixing time of 3.4 ms was used. $^1H\{^{13}C\}$-HMBC spectra utilized gradient selection acquiring 820 t_1 increments with 160 transients of 4096 data points each with a spectral widths in f2 and f1 of 5000 and 25140 Hz, respectively, and a mixing time of 50 ms. A low-pass filter was employed to suppress one bond J_{CH} couplings. All spectra were analyzed and assigned using Topspin 3.2 software (Bruker BioSpin).

Reductive Half-Reaction of Renalase with 2 and 6DHNAD. The reductive half-reaction of renalase could be observed independent of subsequent oxidative processes by exclusion of dioxygen. Renalase (5 mL, 20 μM) in 2 × PBS

DOI: 10.1021/bi5013436
Biochemistry 2015, 54, 795−806

Scheme 2

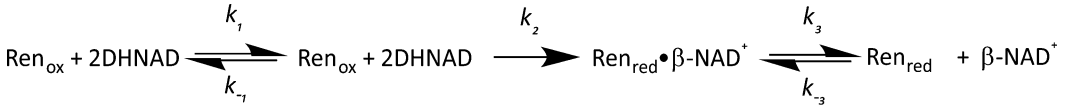

buffer containing 1 mM dextrose was added to the main chamber of a glass tonometer, and glucose oxidase (25 μL, 25 units) was added to a detachable side arm. The tonometer was then assembled and embedded in ice, and the renalase and glucose oxidase solutions were made anaerobic by exchanging argon for dissolved dioxygen. This was achieved by 45 alternating cycles of low-level vacuum followed by the introduction high-purity argon gas (at 5 psi). The argon was passed through an Alltech oxygen-reactive cartridge and sparged through anaerobic water. Throughout this procedure the sample was equilibrated with the argon atmosphere by gentle agitation after each set of three exchange cycles. Once anaerobic, the glucose oxidase was combined with the renalase/dextrose solution and mounted onto a Hitech (now TgK) DX2 stopped flow instrument. 6DHNAD samples were thawed (see above) and diluted to target concentrations in water containing 1 mM dextrose. Each 6DHNAD sample was then placed in a glass syringe, inverted, and sparged with argon gas for 5 min. Before capturing and mounting the substrate solution to the stopped flow instrument, 10 μL of glucose oxidase (10 units) was injected via the luer tip. 2DHNAD substrate solutions were prepared in an equivalent manner but were collected directly from preparative HPLC purification (50−90 μM) and used immediately (see above).

Renalase and substrate solutions were mixed, and reduction of the renalase cofactor was observed at 458 nm. The stability of 6DHNAD substrate allowed it to be prepared in sufficient concentrations to achieve pseudo-first-order reaction conditions. As such the data for this substrate were fit to a linear combination of two exponentials according to eq 1 using Kinetic Studio software (TgK Ltd.). In this equation A_1 and A_2 are the amplitudes associated with the first and second rate constants, k_{1obs} and k_2, and C is the absorbance at end of the reaction. The dependence of the k_{1obs} values determined was then fit to the hyperbolic form of the single-site binding equation (eq 2) according to Strickland, where k_{red} is the limiting rate constant for reduction and K_{6DHNAD} is the dissociation constant for 6DHNAD.[23]

$$A_{458} = A_1(e^{-k_{1obs}t}) + A_2(e^{-k_2t}) + C \quad (1)$$

$$k_{obs} = \frac{k_{red}[6DHNAD]}{(K_{6DHNAD} + [6DHNAD])} \quad (2)$$

For 2DHNAD, 100 μM was the approximate maximum concentration obtained from preparative HPLC; as such, the reductive half-reaction with this substrate was conducted under second-order reactant conditions and the data obtained were fit globally using Kintec Explorer to the model shown in Scheme 2. In this model the Ren_{ox}·2DHNAD complex k_{on} rate constant was arbitrarily assigned to $\sim 10^8$ M^{-1} s^{-1}, and the ratio of the k_3 and k_{-3} for the Ren_{red}·β-NAD^+ complex was confined to equal the measured dissociation constant for the Ren_{ox}·β-NAD^+ complex (for justification, see below).

Dissociation Constants for the Ren_{ox}·β-NADH and Ren_{ox}•β-NAD^+ Complexes. The dissociation constants for the Ren_{ox}·β-NADH and Ren_{ox}·β-NAD^+ complexes were measured by perturbation of the renalase flavin spectrum in the presence of each ligand. In order to avoid slow nonspecific reduction of the renalase flavin by β-NADH during the experiment, a ~10 mL stock of renalase (15 μM) was prepared in PBS buffer at 25 °C. From this stock a 0.9 mL aliquot was added to a 1.5 mL quartz cuvette and 0.1 mL of β-NADH was added to this sample from a set of eight 2-fold serially diluted stocks. As such the spectrophotometric data are compiled from eight separate renalase samples observed shortly after the addition of β-NADH for concentrations that spanned the range 0−3.51 mM. The dissociation constant for the Ren_{ox}·β-NAD^+ complex was measured by preparing a single 20 μM solution of renalase in PBS buffer at 25 °C. To this solution β-NAD^+ was titrated such that a range of concentrations from 0 to ~ 6 mM was achieved (higher concentrations induced marked precipitation of the enzyme).

For both β-NADH and β-NAD^+ titrations, spectra (250−900 nm) were acquired for each ligand concentration using a Shimadzu 1800 spectrophotometer. After correction for dilution, the change in absorption at 550 and 500 nm was used to determine the dissociation constant for the Ren_{ox}·β-NADH and the Ren_{ox}·β-NAD^+ complexes, respectively. The changes in absorbance were fit to the hyperbolic form of the single site binding equation (eq 3) in which f is fractional saturation and K_{ligand} is the dissociation constant for either β-NADH or β-NAD^+ for the respective Ren_{ox} complex.

$$f = \frac{[ligand]}{(K_{ligand} + [ligand])} \quad (3)$$

2- and 6DHNAD Dehydrogenase Inhibition. Inhibition of dehydrogenases from primary metabolism by 2- and 6DHNAD was assessed using two approaches. The relative stability of 6DHNAD allowed the collection of a series of nested Michealis-Menten curves each acquired in the presence of a different concentration of the candidate inhibitor. The relative instability of 2DHNAD dictated that the 50% inhibitory concentration (IC50) method of Cheng and Prusoff was used for determination of K_i.[24,25] Via this approach, 2DHNAD need only be separated from 6DHNAD and β-NADH using preparative HPLC, quantified, and diluted to the target concentration before adding to the assay; as such the pure 2DHNAD is used within 5 min of purification.

6DHNAD and 2DHNAD K_i values were measured for three dehydrogenase enzymes of primary metabolism: malate dehydrogenase (MDH), lactate dehydrogenase (LDH), and lipoamide dehydrogenase (DLD). To limit the influence of enzyme instability encountered with the MDH and LDH enzymes, a solution of 0.3 U/mL was prepared in 10 mM potassium phosphate pH 7.5 and then frozen at −80 °C as 2 mL aliquots. These samples were then thawed and used as required. By contrast, DLD (0.3 U/mL) maintained activity when incubated at 4 °C and so was prepared in 100 mM potassium phosphate pH 7.5 and placed on ice until used in assays. For assessment of 6DHNAD inhibition of MDH and LDH, a series of five Michaelis−Menten analyses were completed using β-NADH concentrations from 0 to 80 μM

DOI: 10.1021/bi5013436
Biochemistry 2015, 54, 795−806

in the presence of saturating respective oxaloacetate (0.4 mM) and pyruvate (0.5 mM). For MDH and DLD, 6DHNAD were varied from 0 to 2 μM, while for LDH the range of 6DHNAD used was 0−20 μM. The data obtained for MDH and LDH were fit globally to the competitive inhibition model using the nonlinear least-squares analysis provided by Prism 6 software (Graphpad Software Inc.).

K_i values for 2DHNAD with MDH, LDH, and DLD were assessed using the IC50 method. In this method the extent of inhibition for a range of 2DHNAD concentrations was measured at a concentration of β-NADH equivalent to the measured Michaelis constant for this substrate. This value was determined in the absence of inhibitor and at near saturating concentrations of the oxidized substrate (0.4 mM oxaloacetate, 0.5 mM pyruvate, 1 mM lipoamide acid for MDH, LDH, and DLD respectively). All data were fit using nonlinear least-squares analysis available from Kalieidagraph software (Synergy Software Inc.). The data obtained in the absence of the inhibitor were fit to eq 4, the Michaelis−Menten equation, where v is the observed rate, V_{max} is the maximal rate of reaction, and $K_{\beta\text{-NADH}}$ is the Michaelis constant for β-NADH. The extent of inhibition was then measured for a range of 2DHNAD concentrations and the data obtained were fit to the Hill equation (eq 5) to derive the IC50 midpoint as a measure of the K_i value for 2DHNAD.

$$v = \frac{V_{max}[\beta\text{-NADH}]}{(K_{\beta\text{-NADH}} + [\beta\text{-NADH}])} \quad (4)$$

$$v = V_{min} + \frac{V_{max} - V_{min}}{\left(1 + \left(\frac{[2DHNAD]}{K_i}\right)\right)} \quad (5)$$

RESULTS

Renalase Substrates are Generated by Non-Specific Reduction of β-NAD$^+$. In prior work we identified small equilibrium proportions of molecules in β-NAD(P)H solutions that were oxidized by renalase. The absorption maxima, extinction coefficients, and apparent equilibrium proportions correlated well with those reported for α-anomers of NAD(P)H molecules, but the fleeting behavior of these molecules precluded rigorous structural assignment. We have since devised methods to both form larger fractional accumulations of these molecules by reduction of β-NAD$^+$ and prolong the decay half-life such that structural assignments can be made. Figure 1A illustrates the chromatographic separation of the reduced products obtained when β-NAD$^+$ is reduced by either hydrosulfite and borohydride. While hydrosulfite (E° = −0.62 V) yields only β-NADH (4DHNAD), reduction by borohydride (E° = −1.24 V) yields three products, two of which are substrates for renalase (Figure 1B). The third component, that was not a substrate for renalase, had a retention time identical to that of β-NADH. When reacted with renalase, the product from both substrate molecules was identified here (and in prior work) as β-NAD$^+$, and this product was made in near equimolar concentration to the amount of dioxygen consumed (Figure 1B inset).[18] The absorption spectra of the reduction products indicate distinct UV/vis maxima at 345, 394, and 340 nm for the dihydro-nicotinamide moiety in each case (Figure 1C).

Structural Assignment of Renalase Substrates. The unique absorption maxima of each borohydride reduction

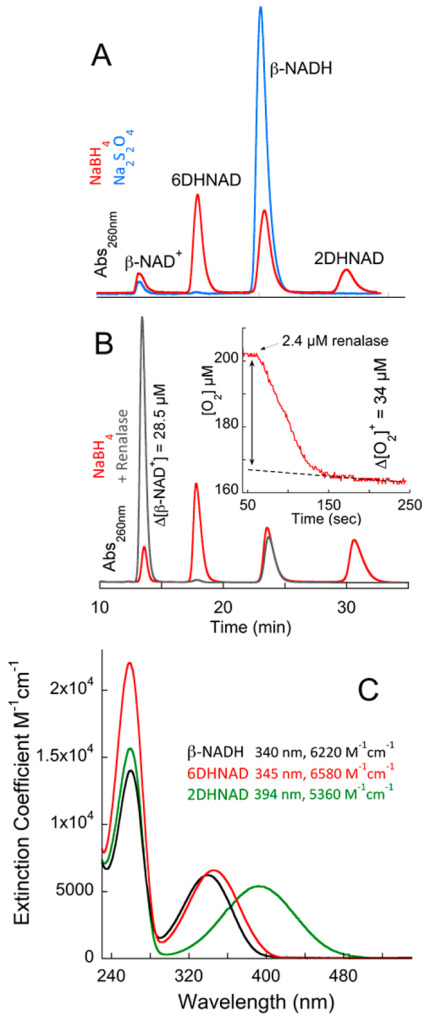

Figure 1. Generation of renalase substrates by reduction of β-NAD$^+$. (A) Analytical HPLC chromatograms recorded after the reduction of 50 μM β-NAD$^+$ with 50 μM sodium hydrosulfite (blue line) or 50 μM sodium borohydride (red line). (B) Analytical HPLC chromatograph demonstrating the consumption of two of the three products of sodium borohydride reduction by the addition of 2.4 μM renalase. The inset is taken from observation of the reaction shown in B using a Clark-type dioxygen electrode. After cessation of dioxygen consumption (~100 s), the sample was filtered using an Amicon 0.5 mL 10 kDa centrifugal filtration device and rechromatographed as described (gray vs red chromatogram). (C) Molar absorptivity absorption spectra of the purified reduction products.

product were used to aid isolation of sufficient quantities by preparative HPLC for structural characterization. The mass of all reduction products was found to be 664.40 ± 0.05, equal to the mass of the β-NADH control. The mass of the product formed from renalase activity was 662.40 ± 0.00, equivalent to that of the β-NAD$^+$ control. NMR spectra were recorded at 280 K in D_2O solvent. For each product, one-dimensional H^1 (1D), H^1 homonuclear correlation (COSY), H^1−C^{13} heteronuclear single quantum coherence (HSQC) and H^1−C^{13} heteronuclear multiple bond correlation (HMBC) spectra were obtained. Chemical shift and H^1 coupling assignments are included in Table S1 in the Supporting Information section. Figure 2 depicts the proton resonances assigned to the dihydronicotinamide rings of three products obtained from borohydride reduction. In terms of homonuclear H^1 geminal and vicinal coupling, nicotinamide dinucleotides have four isolated sets of

DOI: 10.1021/bi5013436
Biochemistry 2015, 54, 795−806

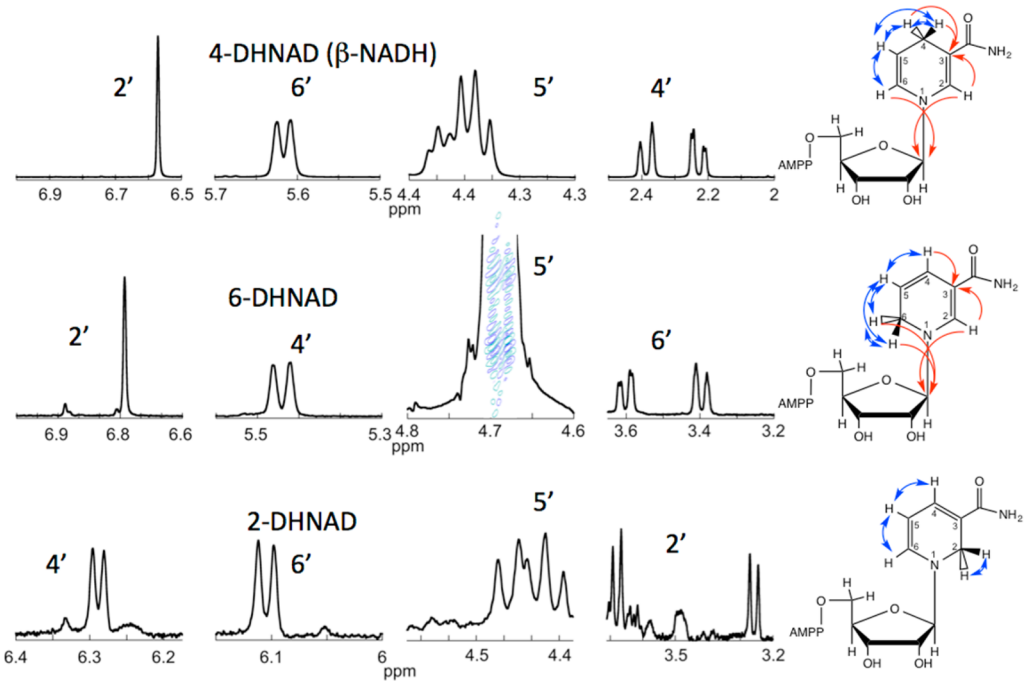

Figure 2. NMR identification of the purified products of sodium borohydride reduction of β-NAD$^+$. Spectra were recorded at 280 K in deuterium oxide. Structures to the right depict the primary couplings used for identification of the β-NADH isomers. Blue arrows indicate homonuclear coupling, while red arrows indicate heteronuclear multibond coupling.

protons; those for the adenine and nicotinamide bases and two for the ribose moieties. Structural assignment of the nicotinamide bases therefore relies heavily on HMBC spectra to link the proton residing on the ribose anomeric carbon to the proximal N2 and N6 carbons and/or the protons residing on N2 and N6 to the anomeric carbon. These multibond heteronuclear couplings both orient the nicotinamide nuclear spin-system with respect to the ribose and also permit deconvolution of the individual ribose resonances that are then identified by sequential geminal homonuclear coupling. The pivotal geminal, vicinal homonuclear couplings, and heteronuclear multiple bond couplings are indicated in Figure 2 by respective blue and red arrows. Correlations of this type were readily made for the 340 and 345 nm absorption maxima species, and these were assigned as 4- (β-NADH) and 6DHNAD respectively (Figure 2A,B). Note that the multiplet for the nicotinamide N5′ proton of 6DHNAD is obscured by the residual water resonance and is instead depicted inset as the homonuclear coupling crosspeak to the N6′ protons. The relative instability of the reduction product that exhibited the 394 nm absorption maximum precluded obtaining assignments by this approach. Control H^1 1D NMR spectra taken before and after two-dimensional heteronuclear spectra acquisition repeatedly indicated substantial degradation of the 394 nm species. As such the structural assignment of the 394 nm species as 2DHNAD is principally based on H^1 homonuclear couplings. For this species we observe a ∼6−7 Hz geminal coupling for the N4′(d), N5′(m), and N6′(d) protons and an absence of geminal couplings in the resonances assigned to N2′ protons that each exhibit only a vicinally coupled ∼12 Hz doublet (Figure 2C, Table S1, Supporting Information).

Renalase Reductive Half-Reaction. In prior work we published data for the reductive half-reaction of renalase.[7] In these experiments the substrate was supplied to the enzyme in an apparent equilibrium mixture arising from aqueous speciation of β-NADPH (Scheme S1, Supporting Information). As such the data obtained were not for a pure substrate molecule and included potential competitive inhibition effects from the β-NADPH background (see below). Here we show the reductive half-reactions for renalase with pure 2- and 6DHNAD. While 6DHNAD has sufficient stability to be purified and stored for use in such experiments, 2DHNAD does not and typically decomposes with a half-life of approximately 30 min. For this reason 2DHNAD was used immediately after preparative HPLC isolation and was limited to ∼100 μM concentration by the capacity to resolve 2DHNAD from other reduction products with the preparative reverse-phase phenyl HPLC column used for purification. To observe reduction of the renalase flavin cofactor by 2- and 6DHNAD, anaerobic renalase (10 μM final) was mixed with varied concentrations of the anaerobic substrates. For 6DHNAD the range of substrate concentration used spanned approximate pseudo-first-order reactant ratios (50−800 μM). The data obtained were thus fit to exponential decay(s) (eq 1). Two phases were observed in the reduction traces. The first phase accounted for ∼90% of the amplitude change and was indicative of flavin reduction. The rate constants for this phase (k_{1obs}) derived from fitting displayed a hyperbolic dependence that was fit to eq 2 to derive the limiting rate constant for reduction from the asymptote (234 s^{-1}) and the dissociation constant for the Ren$_{ox}$·6DHNAD complex (173 μM). The rate constant for the second phase did not exhibit a 6DHNAD dependence and was fit to ∼20 s^{-1} in all traces. We propose that flavin reduction forms the Ren$_{red}$·β-NAD$^+$ complex whose flavin spectrum is altered by the proximity of the flavin and nicotinamide rings. This phase is thus tentatively assigned as the decay of the Ren$_{red}$·β-NAD$^+$ complex with the egress of β-NAD$^+$ from the active site. A complete mechanistic assignment of the reductive half-reaction is beyond the scope of this study.

DOI: 10.1021/bi5013436
Biochemistry 2015, 54, 795−806

Our limited capacity to isolate and stabilize 2DHNAD dictated that the reductive half-reaction for renalase oxidizing this substrate was observed within a range of substrate concentrations that were second-order with respect to the enzyme concentration. As such the data obtained could only be analyzed by fitting the integrated rate expression for a more complete kinetic model as shown in Scheme 2. In this model the ratio of the β-NAD$^+$ dissociation and association rate constants (k_3:k_{-3}) was fixed to that defined by the dissociation constant for the Ren$_{ox}$·β-NAD$^+$ complex. This fitting restriction was based on our prior observation that the β-NAD$^+$ product does not modulate the reduction potential of the flavin cofactor and therefore has equal affinity for the Ren$_{ox}$ and Ren$_{red}$ forms (see below).[7] In addition the reductive step (k_2) in which the hydride equivalent is transferred from 2DHNAD to the flavin was defined as irreversible in accord with the assumption that the difference in reduction potential of these two species is greater than 100 mV (ΔG > −20 kJ/mol). Lastly, the association rate constant for 2DHNAD (k_1) was confined as ~10^8 M^{-1} s^{-1}, close to the limit of diffusion. The fit obtained indicated a k_{red} for 2DHNAD of 860 s^{-1}, 3.6-fold faster than that measured for 6DHNAD but with a similar a dissociation constant of 166 μM.

Dissociation Constants for the Ren$_{ox}$·β-NADH and Ren$_{ox}$·β-NAD$^+$ Complexes. We propose that the metabolic function of renalase is to alleviate inhibition of primary metabolism by oxidizing isomers of β-NAD(P)H molecules that arise through tautomerization and/or nonspecific reduction of β-NAD$^+$ (Scheme 3). As such renalase operates in an environment of near-isosteric nonsubstrate molecules such as β-NAD(P)H and β-NAD(P)$^+$ that are present in considerably higher concentration and presumably inhibitory. In order to gauge selectivity for 2- and 6DHNAD the dissociation constants for the Ren$_{ox}$·β-NADH and Ren$_{ox}$·β-NAD$^+$ complexes were measured using perturbation of the renalase flavin spectrum as physical evidence of association. These data fit well to a single site binding equation (eq 3) and indicated that renalase is only 3-fold selective against β-NADH ($K_{\beta\text{-NADH}}$ = 570 ± 90 μM) (Figure 4A) but is 34-fold selective against β-NAD$^+$ ($K_{\beta\text{-NAD+}}$ = 5960 ± 800 μM) (Figure 4B). Association of β-NADH induced new absorption transitions at long wavelength indicative of charge-transfer presumably made possible by proximity of the dihydronicotinamide and flavin rings[26] (Figure 4A inset).

Scheme 3

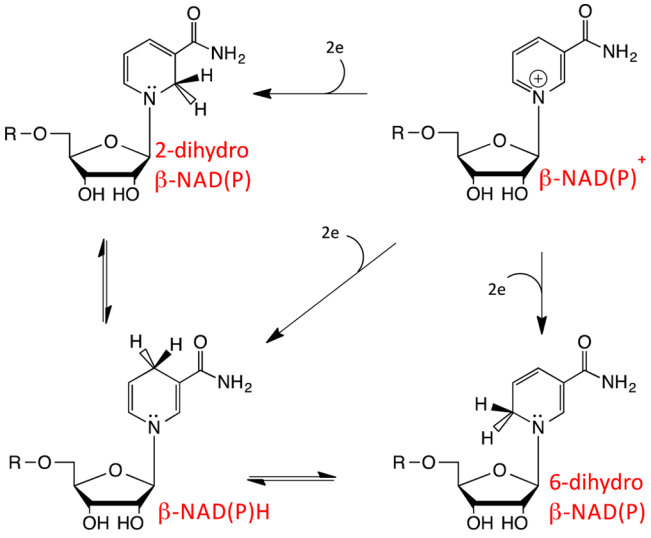

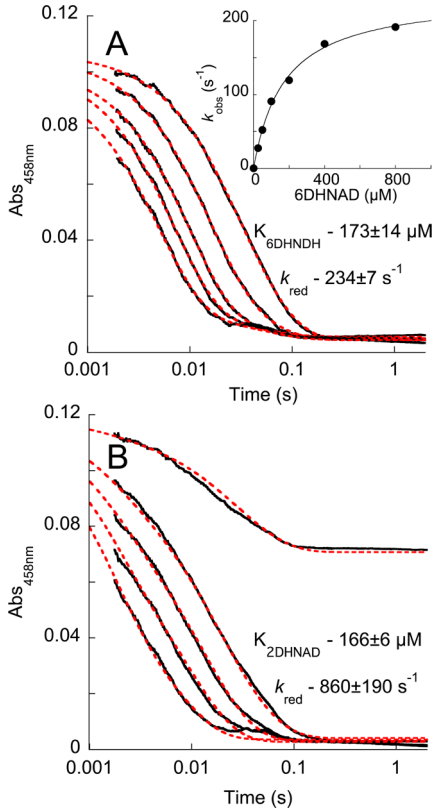

Figure 3. The reductive half-reactions of renalase with 2- and 6DHNAD. (A) Reduction of the renalase cofactor (10 μM) in the presence of 6DHNAD. Traces shown are for 25, 50, 100, 200, 400, and 800 μM 6DHNAD. The data were fit (red dashed lines) to a linear combination of two exponential decays according to eq 1. Inset shows the dependence of the observed rate constants on the concentration of 6DHNAD fit to eq 2. (B) Reduction of the renalase cofactor (10 μM) in the presence of 2DHNAD. Traces shown are for 3.7, 14.5, 21.3, 30.0, 43.5 μM 2DHNAD. These data were fit globally to the kinetic model depicted in Scheme 2.

Dehydrogenase Inhibition. Lowry et al. and Dalziel reported that β-NADH preparations contained contaminants that were inhibitory to LDH,[27,28] and this observation has since been confirmed by numerous other authors.[29−32] In this study we measure K_i values for 2- and 6DHNAD to three dehydrogenase enzymes from primary metabolism. These data are summarized in Figure 5. Predictably, 6DHNAD inhibition was best fit to a competitive pattern with respect to β-NADH. The instability of 2DHNAD precluded categorization of the inhibition pattern, though it can be reasonably assumed that 2DHNAD competes with β-NADH similarly. The data indicate that both 2- and 6DHNAD have high affinity for dehydrogenases and therefore pose a threat to primary metabolism. For *E. coli* MDH, 6DHNAD has exceedingly high affinity (K_i = 34 ± 3 nM), while 2DHNAD has only modest inhibitory affinity for this enzyme (K_i = 3.05 ± 0.33 μM). LDH from rabbit muscle shows similar high affinity for both 2- and 6DHNAD (K_i ≈ 500−600 nM). DLD is a β-NADH-dependent dehydrogenase component of both the pyruvate decarboxylase complex and the α-ketoglutarate decarboxylase complex. Curiously, this dehydrogenase does

DOI: 10.1021/bi5013436
Biochemistry 2015, 54, 795−806

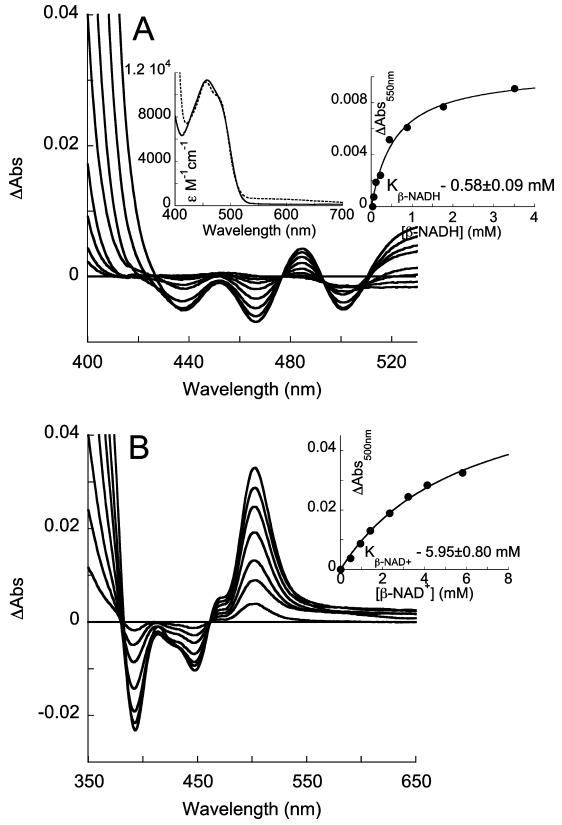

Figure 4. Measurement of the dissociation constants for the Ren_{ox}·β-NADH and Ren_{ox}·β-NAD+ complexes. (A) Difference absorption spectra for the renalase flavin at various concentrations of β-NADH. Inset (left) shows the charge transfer absorption band observed when 3.51 mM β-NADH was added (dashed line) to renalase. Inset (right) depicts the perturbation of the flavin spectrum at 550 nm as a function of β-NADH concentration fit to eq 3. (B) Difference absorption spectra for the renalase flavin at various concentrations of β-NAD^+. Inset depicts the perturbation of the flavin spectrum at 550 nm as a function of β-NADH concentration fit to eq 3.

not appear to bind either 2- or 6DHNAD with significant affinity. Collectively these data establish a credible metabolic function for renalase; oxidation of NAD(P)H isomers that arise from tautomerization or nonspecific reduction of β-$NAD(P)^+$ in order to alleviate stringent inhibition of essential dehydrogenase enzymes.

DISCUSSION

In this report we provide a credible thesis for the metabolic function of renalase. We assert that renalase oxidizes inhibitory isomers of β-NADH, forming β-NAD^+ and delivers the electrons harvested to dioxygen. We offer evidence for the structures of two substrate molecules that arise from nonspecific reduction of β-NAD^+ and present an initial characterization of the kinetics of the reductive half-reaction observed with these substrates. This study also serves to correct our earlier erroneous claim that renalase oxidizes α-NADH molecules.[7,18] The data presented here indicate that the substrate molecule identified in prior work was not α-NAD(P)H but instead 6DHNAD(P), a species that has the same λmax (345 nm), ostensibly the same extinction coefficient, and similar reported aqueous fractional accumulation at equilibrium.[19]

In 1953 Mathews and Conn noted that the β-NADH prepared by borohydride reduction was only partially oxidized by LDH and proposed that in addition to β-NADH (4-DHNAD), 2DHNAD, and 6DHNAD were produced and that these forms were not able to react with enzymes.[33] Later Chaykin and Meissner reported absorption spectra of the partially purified products of borohydride reduction and used tritium label elimination methods to establish the positions of reduction on the nicotinamide ring.[34] A number of other studies have examined the properties of these nonspecific reduction products (including a variety of misidentifications),[29,34−37] but it was Lowry et al. and Dalziel who first reported that β-NADH preparations contained contaminants that were inhibitory to LDH. Soon after, Godtfredsen and Ottesen described 6DHNAD as a humidity-induced lactate dehydrogenase inhibitor that arises in NADH powder.[32,38] Together, these and numerous other studies establish that lactate dehydrogenase inhibitors arise by nonspecific reduction of β-NAD^+ and/or via tautomerization of β-NADH (Scheme 3). The activity we have observed for renalase suggests that nonenzymatic redox and/or proton-movement mediated intercoversion of NAD(P)+/NAD(P)H isomers is also an in vivo phenomenon that suppresses primary metabolism.

We also show that renalase catalytically oxidizes both known isomeric forms of the β-NAD(P)H nicotinamide ring. Positionally, the 2 and 6 carbons of the nicotinamide ring are equivalent if the base is allowed to pivot about the glycosidic bond. This suggests that the nicotinamide amide substituent can be accommodated in two locations within the renalase active site and in these two binding modes the substrates are otherwise conformationally equivalent. Two orientations for the nicotinamide base implies there are also two binding modes for β-NAD(P)H and for β-$NAD(P)^+$ and that the dissociation constant measured for these molecules is an average of both binding modes. Moreover, it also follows that up to half of the binding events for 2- and 6DHNAD result in inhibitory complexes that cannot transfer the hydride equivalent to the renalase flavin; that we do not observe any inhibitory delay in the reductive half reaction suggests that binding and release of 2- and 6DHNAD from Ren_{ox} is rapid.

In prior studies we observed the reductive half-reaction of renalase by mixing the enzyme with an apparent equilibrium mixture of β-NADH and 6DHNAD.[7] Here we use pure preparations of 2DHNAD and 6DHNAD to show that the rate constant for reduction is dramatically more rapid than previously reported. We observe rate constants for flavin reduction of 230 s^{-1} for 6DHNAD and 860 s^{-1} for 2DHNAD as opposed to ∼40 s^{-1} observed with the equilibrium mixture. We also show that renalase has only a modest ability to distinguish between the 2-, 4-, and 6DHNAD molecules (Figures 3 and 4) as β-NADH (4DHNAD) binds to renalase forming a complex with a dissociation constant of ∼600 μM, only ∼3.5-fold weaker than that observed for 2- and 6DHNAD. However, renalase has a considerably greater capacity to distinguish between its substrates and β-$NAD(P)^+$ molecules, the renalase complex(es) of which has an order of magnitude higher dissociation constant (Figure 4B).[7] As such the relative high background of β-NAD(P)H and β-$NAD(P)^+$ in the cellular environment will populate and inhibit renalase to some extent. Given the ostensibly isosteric form of all three reduced isomers, it is not unexpected that β-NAD(P)H would compete for access to the renalase active site. The apparent lack of β-NAD(P)H isomer binding stringency is only a limitation to the

DOI: 10.1021/bi5013436
Biochemistry 2015, 54, 795−806

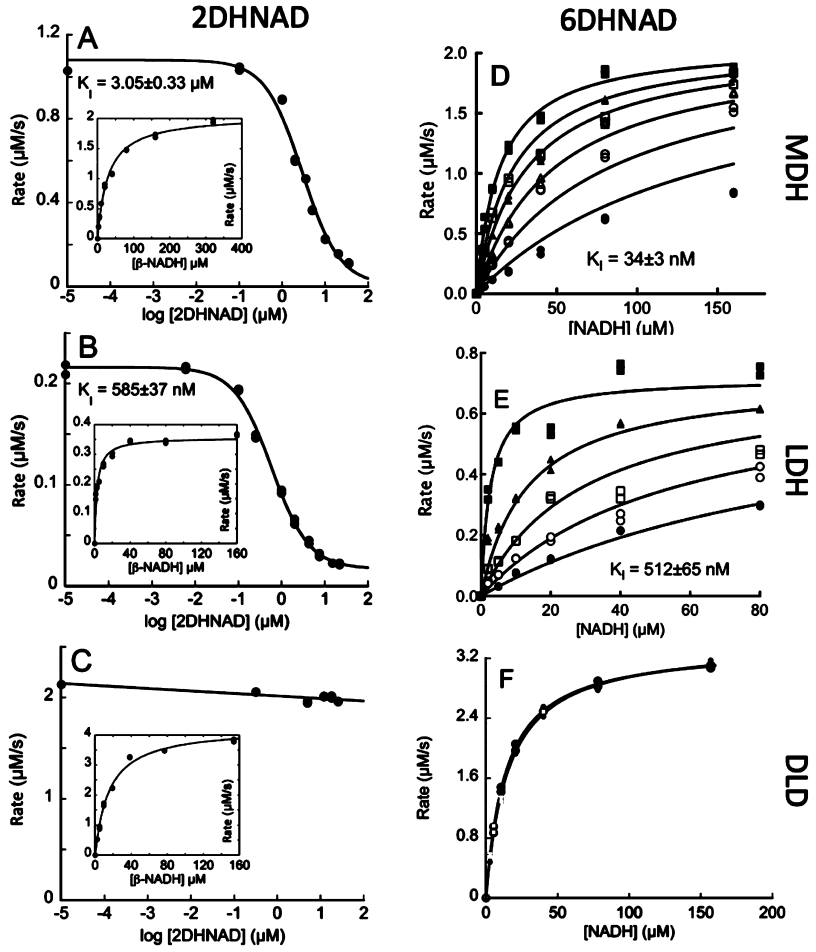

Figure 5. Inhibition of dehydrogenases from primary metabolism by 2- and 6DHNAD. Panels A and D depict evidence for the inhibition of *E. coli* malate dehydrogenase by 2DHNAD and 6DHNAD, respectively. In D the 6DHNAD concentrations used were 0, 20, 40, 80, 160, 320 nM. Panels B and E depict evidence for the inhibition of porcine heart lactate dehydrogenase by 2DHNAD and 6DHNAD. In panel E the 6DHNAD concentrations used were 0, 2, 5, 10, 20 μM. Panels C and F depict evidence for the absence of inhibition of *rabbit muscle* lipoamide dehydrogenase by 2DHNAD and 6DHNAD respectively.

extent that 2- and 6DHNAD accumulate in vivo. The considerable driving force for the renalase reaction derived from the reduction of dioxygen provides a rather unrelenting capacity to scavenge these substrates. Provided renalase activity can scavenge both isomers at a rate that meets or exceeds their formation, its metabolic contribution is sufficient.

We have assessed the interaction of 2- and 6DHNAD with three dehydrogenases from primary metabolic pathways. 2- and 6DHNAD presumably act as inhibitors of these enzymes as they are highly similar in shape and electrostatic character to β-NADH, yet cannot associate in a manner that permits hydride transfer. These data indicate that both MDH and LDH are subject to inhibition by both 2- and 6DHNAD while DLD is not. Given the structural similarity of 2-, 4-, and 6DHNAD, it is interesting that DLD can select only the 4-dihydro isomer, while renalase, the enzyme apparently destined to rid the cell of 2- and 6DHNAD, cannot. The inhibition of MDH by 6DHNAD is an order of magnitude more potent suggesting that this interaction is the principal threat to primary metabolism from β-NAD(P)H isomers. While the in vivo concentrations of 2- and 6DHNAD are not known, such high affinity would suggest that, in the absence of renalase, even minute accumulations of 6DHNAD would undermine primary energy pathways. While 2-DHNAD is much less stable than 6DHNAD, on a molecular time scale its half-life is more than sufficient to expect that it will also exert an influence over key dehydrogenase enzymes. The extent of the threat these molecules pose is likely to be organism specific, and it cannot yet be stated that dehydrogenase inhibition of this type is a universal phenomenon. That porcine DLD is not inhibited by either 2- or 6DHNAD indicates that binding selectivity for these three forms of reduced β-NADH is possible. However, renalase is found throughout the *animalia* implying that key dehydrogenases found within all organisms of this kingdom, such as rabbit LDH shown here, are subject to inhibition by β-NADH isomers.

As stated, in prior work we mistakenly proposed that α-NAD(P)H anomers were substrates for renalase. It now seems appropriate to graft our earlier mechanistic observations with the data obtained in this study using pure 2- and 6DHNAD. Scheme 4 depicts the proposed mechanism for renalase based on prior and current observations. For simplicity this scheme depicts only the catalytic cycle for the 6DHNAD substrate, though it is assumed that catalysis in the presence of 2DHNAD differs only in the position of the nicotinamide amide substituent (meta with respect to the position depicted). In this catalytic cycle 6DHNAD associates rapidly with a dissociation constant for the Ren$_{ox}$·β-6DHNAD(P) complex

DOI: 10.1021/bi5013436
Biochemistry 2015, 54, 795−806

Scheme 4

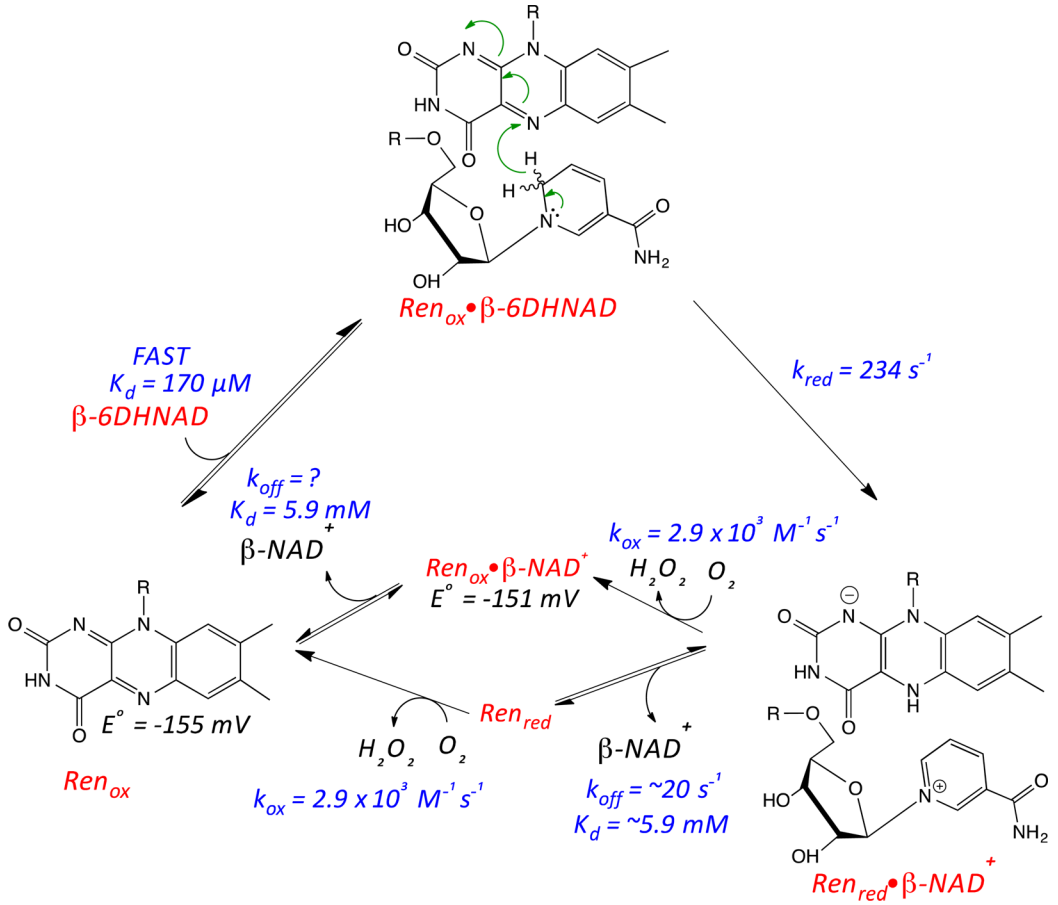

of 170 μM. The nicotinamide locates in the active site such that the ortho positions with respect to the dihydropyridyl nitrogen are adjacent to the flavin N5 and oriented for conventional hydride transfer. Reduction of the flavin forms the Ren$_{red}$·β-NAD(P)$^+$ complex. Our prior studies indicated that the reoxidation of this complex occurs by a bimolecular reaction with dioxygen with a rate constant of 2.9 × 10^3 M^{-1} s^{-1} that forms hydrogen peroxide and is fully rate determining under conditions of normal mammalian physiological oxygen concentration (~140 μM).[7] The rate constant for reoxidation was not influenced by the addition of exogenous β-NAD(P)$^+$ indicating that the reaction with dioxygen is neither contingent on nor influenced by the release of β-NAD(P)$^+$. Consistent with this observation was that the reduction potential of the renalase flavin is the same within error for the unliganded oxidized enzyme and the Ren$_{red}$·β-NAD(P)$^+$ complex.[7] As such the reoxidation/product release phase of catalysis is represented as random but is kinetically ordered by the fact that β-NAD(P)$^+$ is released somewhat more rapidly (20 s^{-1}) than the reaction of the reduced enzyme with dioxygen under physiological conditions (0.4 s^{-1}).

The number and breadth of physiological observations associated with renalase are expanding in an exponential manner. In addition to being linked to the control of blood pressure and heart rate,[1,39] renalase has also been associated with renal dopamine and phosphate metabolism,[10,12] diabetes,[11,40,41] and amelioration of myocardial damage.[42] Our earlier conclusions were based on recycling of α-anomers of NAD(P)H molecules and could not be linked to any known endocrine or other physiological role for renalase. While we make no attempt here to connect our current data to specific physiological responses, it does seem that the threat to normal primary metabolism posed by β-NAD(P)H isomers does allow for renalase deficiencies to manifest as physiological abnormalities, in particular those associated with local ischemia.

■ ASSOCIATED CONTENT

Supporting Information

Table S1 that includes NMR shift assignments for the three reduced forms of β-NADH described in this manuscript; a scheme that depicts the known modes of β-NAD(P)H aqueous speciation. This scheme is provided as a summary reference. This material is available free of charge via the Internet at http://pubs.acs.org.

■ AUTHOR INFORMATION

Corresponding Author

*Phone: (414) 940 0059. Fax: (414) 229 5530. E-mail: moran@uwm.edu.

Funding

This research was supported by a National Science Foundation grant to G.R.M (CHE-1402475) and by a University of Wisconsin-Milwaukee Research Growth Initiative Grant to G.R.M.

Notes

The authors declare no competing financial interest.

DOI: 10.1021/bi5013436
Biochemistry 2015, 54, 795−806

■ ABBREVIATIONS

HPLC, high performance liquid chromatography; FAD, flavin adenine dinucleotide; β-NADPH, reduced nicotinamide adenine dinucleotide phosphate; β-NADH (4DHNAD), reduced nicotinamide adenine dinucleotide; β-NAD^+, oxidized nicotinamide adenine dinucleotide; 2DHNAD, 2-dihydronicotinamide adenine dinucleotide; 6DHNAD, 6-dihydronicotinamide adenine dinucleotide[a]; IPTG, isopropyl-β-thioglactopyranoside; HEPES, 2-[4-(2-hydroxyethyl)piperazin-1-yl]-ethanesulfonic acid; β-ME, beta-mercaptoethanol; MDH, malate dehydrogenase; LDH, lactate dehydrogenase; DLD, lipoamide dehydrogenase; OYE, old yellow enzyme; IC50, 50% inhibitory concentration

■ ADDITIONAL NOTE

[a]The naming convention used throughout this article is based on common usage for reduced nicotinamide bases. Early naming of reduced NAD(P) molecules used 1,2-, 1,4-, or 1,6-dihydroNAD. However, reduced nicotinamides gain only a single hydrogen at the position of reduction and are therefore formally 2, 4, or 6-monohydronicotinamides. We have chosen instead the descriptive hybrid name of *n*-dihydronicotinamide (n-DHNAD) based on the current convention of describing the reduced pyridyl ring of NAD as a dihydropyridyl moiety.

■ REFERENCES

(1) Xu, J., Li, G., Wang, P., Velazquez, H., Yao, X., Li, Y., Wu, Y., Peixoto, A., Crowley, S., and Desir, G. V. (2005) Renalase is a novel, soluble monoamine oxidase that regulates cardiac function and blood pressure. *J. Clin. Invest.; 115*, 1275−1280.

(2) Li, G., Xu, J., Wang, P., Velazquez, H., Li, Y., Wu, Y., and Desir, G. V. (2008) Catecholamines regulate the activity, secretion, and synthesis of renalase. *Circulation 117*, 1277−1282.

(3) Hennebry, S. C., Eikelis, N., Socratous, F., Desir, G., Lambert, G., and Schlaich, M. (2010) Renalase, a novel soluble FAD-dependent protein, is synthesized in the brain and peripheral nerves. *Mol. Psychiatr. 15*, 234−236.

(4) Fedchenko, V., Globa, A., Buneeva, O., and Medvedev, A. (2013) Renalase mRNA levels in the brain, heart, and kidneys of spontaneously hypertensive rats with moderate and high hypertension. *Med. Sci. Monit. Basic Res. 19*, 267−270.

(5) Fedchenko, V. I., Kaloshin, A. A., Mezhevikina, L. M., Buneeva, O. A., and Medvedev, A. E. (2013) Construction of the coding sequence of the transcription variant 2 of the human renalase gene and its expression in the prokaryotic system. *Int. J. Mol. Sci. 14*, 12764−12779.

(6) Milani, M., Ciriello, F., Baroni, S., Pandini, V., Canevari, G., Bolognesi, M., and Aliverti, A. (2011) FAD-binding site and NADP reactivity in human renalase: a new enzyme involved in blood pressure regulation. *J. Mol. Biol. 411*, 463−473.

(7) Beaupre, B. A., Hoag, M. R., Carmichael, B. R., and Moran, G. R. (2013) Kinetics and equilibria of the reductive and oxidative half-reactions of human renalase with alpha-NADPH. *Biochemistry 52*, 8929−8937.

(8) Malyszko, J., Koc-Zorawska, E., Malyszko, J. S., Kozminski, P., Zbroch, E., and Mysliwiec, M. (2012) Renalase, stroke, and hypertension in hemodialyzed patients. *Renal Failure 34*, 727−731.

(9) Przybylowski, P., Koc-Zorawska, E., Malyszko, J. S., Mysliwiec, M., and Malyszko, J. (2013) Renalase and endothelial dysfunction in heart transplant recipients. *Transplant Proc. 45*, 394−396.

(10) Zbroch, E., Koc-Zorawska, E., Malyszko, J., and Mysliwiec, M. (2013) Circulating levels of renalase, norepinephrine, and dopamine in dialysis patients. *Renal Failure 35*, 673−679.

(11) Guo, X., Wang, L., Velazquez, H., Safirstein, R., and Desir, G. V. (2014) Renalase: its role as a cytokine, and an update on its association with type 1 diabetes and ischemic stroke. *Curr. Opin. Nephrol. Hypertens. 23*, 513−518.

(12) Sizova, D., Velazquez, H., Sampaio-Maia, B., Quelhas-Santos, J., Pestana, M., and Desir, G. V. (2013) Renalase regulates renal dopamine and phosphate metabolism. *Am. J. Physiol. Renal Physiol. 305*, F839−844.

(13) Lee, H. T., Kim, J. Y., Kim, M., Wang, P., Tang, L., Baroni, S., D'Agati, V. D., and Desir, G. V. (2013) Renalase protects against ischemic AKI. *J. Am. Soc. Nephrol. 24*, 445−455.

(14) Baroni, S., Milani, M., Pandini, V., Pavesi, G., Horner, D., and Aliverti, A. (2013) Is renalase a novel player in catecholaminergic signaling? The mystery of the catalytic activity of an intriguing new flavoenzyme. *Curr. Pharm. Des. 19*, 2540−2551.

(15) Dziedzic, M., Petkowicz, B., Bednarek-Skublewska, A., Solski, J., Buczaj, A., and Choina, P. (2014) Relationship between renalase and N-terminal pro-B-type natriuretic peptide (NT pro-BNP) in haemodialysis patients. *Ann. Agric Environ. Med. 21*, 132−135.

(16) Wang, S., Lu, X., Yang, J., Wang, H., Chen, C., Han, Y., Ren, H., Zheng, S., He, D., Zhou, L., Asico, L. D., Wang, W. E., Jose, P. A., and Zeng, C. (2014) Regulation of renalase expression by D5 dopamine receptors in rat renal proximal tubule cells. *Am. J. Physiol. Renal Physiol. 306*, F588−596.

(17) Desir, G. V., Wang, L., and Peixoto, A. J. (2012) Human renalase: a review of its biology, function, and implications for hypertension. *J. Am. Soc. Hypertens. 6*, 417−426.

(18) Beaupre, B. A., Carmichael, B. R., Hoag, M. R., Shah, D. D., and Moran, G. R. (2013) Renalase Is an alpha-NAD(P)H Oxidase/Anomerase (JACS Spotlight Article). *J. Am. Chem. Soc. 135*, 13980−13987.

(19) Klemm, A., Steiner, T., Flotgen, U., Cumme, G. A., and Horn, A. (1997) Determination, purification, and characterization of alpha-NADH and alpha-NADPH. *Method Enzymol. 280*, 171−186.

(20) Oppenheimer, N. J., and Kaplan, N. O. (1975) The alpha beta epimerization of reduced nicotinamide adenine dinucleotide. *Arch. Biochem. Biophys. 166*, 526−535.

(21) Oppenheimer, N. J. (1982) Chemistry and Solution Confromation of Pyridine Nucleotides, In *The Pyridine Nucletide coenzymes* (Everse, J., Anderson, B., and You, K.-S., Eds.) pp 51−90, Academic Press Inc., New York.

(22) Pace, N. C., Vajdos, F., Fee, L., Grimsley, G., and Gray, T. (1995) How to measure and predict the molar absorption coefficient of a protein. *Protein Sci. 4*, 2411−2423.

(23) Strickland, S., Palmer, G., and Massey, V. (1975) Determination of dissociation constants and specific rate constants of enzyme-substrate (or protein-ligand) interactions from rapid reaction kinetic data. *J. Biol. Chem. 250*, 4048−4052.

(24) Cheng, Y., and Prusoff, W. H. (1973) Relationship between the inhibition constant (K1) and the concentration of inhibitor which causes 50% inhibition (I50) of an enzymatic reaction. *Biochem. Pharmacol. 22*, 3099−3108.

(25) Cortes, A., Cascante, M., Cardenas, M. L., and Cornish-Bowden, A. (2001) Relationships between inhibition constants, inhibitor concentrations for 50% inhibition and types of inhibition: new ways of analysing data. *Biochem. J. 357*, 263−268.

(26) Crozier-Reabe, K. R., Phillips, R. S., and Moran, G. R. (2008) Kynurenine 3-monooxygenase from Pseudomonas fluorescens: substrate-like inhibitors both stimulate flavin reduction and stabilize the flavin-peroxo intermediate yet result in the production of hydrogen peroxide. *Biochemistry 47*, 12420−12433.

(27) Lowry, O. H., Passonneau, J. V., and Rock, M. K. (1961) The stability of pyridine nucleotides. *J. Biol. Chem. 236*, 2756−2759.

(28) Dalziel, K. (1963) The purification of nicotinamide adenine dinucleotide and kinetic effects of nucleotide impurities. *J. Biol. Chem. 238*, 1538−1543.

(29) Chakraverty, K., and Chaykin, S. (1964) 1,6 DPNH, an enzymatically active form of reduced DPN. *Biochem. Biophys. Res. Commun. 15*, 262−268.

DOI: 10.1021/bi5013436
Biochemistry 2015, 54, 795−806

(30) Biellmann, J. F., Lapinte, C., Haid, E., and Weimann, G. (1979) Structure of lactate dehydrogenase inhibitor generated from coenzyme. *Biochemistry 18*, 1212−1217.
(31) Wenz, I., Loesche, W., Till, U., Petermann, H., and Horn, A. (1976) Purification and characterization of commercial NADH and accompanying dehydrogenase inhibitors. *J. Chromatogr. 120*, 187−196.
(32) Godtfredsen, S. E., and Ottesen, M. (1978) 1,6-Dihydro-NAD as an Humidity-Induced Lactate Dehydrogenase Inhibitor in NADH Preparations. *Carlesberg Res. Comm 43*, 171−175.
(33) Mathews, M. B., and Conn, E. E. (1953) The Reaction of Diphosphopyridine Nucleotide with Sodium Borohydride. *J. Am. Chem. Soc. 75*, 5428−5430.
(34) Chaykin, S., and Meissner, L. (1964) The borohydride reduction products of DPN. *Biochem. Biophys. Res. Commun. 14*, 233−240.
(35) Chakraverty, K., King, L., Watson, J. G., and Chaykin, S. (1969) Reduced 1,6-dihydrodiphosphopyridine nucleotide. Chemical properties and enzymatic modification. *J. Biol. Chem. 244*, 4208−4217.
(36) Chaykin, S., Chakraverty, K., King, L., and Watson, J. G. (1966) Tritium-labeled DPN+ and TPN+. *Biochim. Biophys. Acta 124*, 1−12.
(37) Chaykin, S., King, L., and Watson, J. G. (1966) The reduction of DPN+ and TPN+ with sodium borohydride. *Biochim. Biophys. Acta 124*, 13−25.
(38) Godtfredsen, S. E., Ottesen, M., and Andersen, N. R. (1979) On the Mode of Formation of 1,6-Dihydro-NAD in NADH Preparations. *Carlesberg Res. Comm 44*, 65−75.
(39) Desir, G. V. (2007) Renalase is a novel renal hormone that regulates cardiovascular function. *J. Am. Soc. Hypertens. 1*, 99−103.
(40) Koc-Zorawska, E., Malyszko, J., Zbroch, E., and Mysliwiec, M. (2012) Vascular adhesion protein-1 and renalase in regard to diabetes in hemodialysis patients. *Arch Med. Sci. 8*, 1048−1052.
(41) Buraczynska, M., Zukowski, P., Buraczynska, K., Mozul, S., and Ksiazek, A. (2011) Renalase gene polymorphisms in patients with type 2 diabetes, hypertension and stroke. *Neuromol. Med. 13*, 321−327.
(42) Wu, Y., Xu, J., Velazquez, H., Wang, P., Li, G., Liu, D., Sampaio-Maia, B., Quelhas-Santos, J., Russell, K., Russell, R., Flavell, R. A., Pestana, M., Giordano, F., and Desir, G. V. (2011) Renalase deficiency aggravates ischemic myocardial damage. *Kidney Int. 79*, 853−860.

DOI: 10.1021/bi5013436
Biochemistry 2015, 54, 795−806